Impact of High Altitude Low Pressure Environments on Fire Smoke Propagation in Highway Tunnels

Shunheng Hua[1*] , Xinru Tong[1] , Qiang Qu[2] , Yang Xu[1]

[1] School of Energy & Environment, Zhongyuan University of Technology, Zhengzhou 450007, China
[2] Chemical, Mineral and Petroleum Laboratory, Zhanjiang Customs Technology Center, Zhanjiang 524018, China

Corresponding Author Email: 2021108309@zut.edu.cn

ABSTRACT

The distinct characteristics of high-altitude regions, such as lower atmospheric pressure, reduced air density, diminished oxygen content, and cooler environmental temperatures, significantly influence the nature of tunnel fires. This study employs the Fire Dynamics Simulator (FDS) to simulate highway tunnel fires under five different ambient pressure scenarios. Utilizing dual heat sources of three powers 5MW, 10MW, and 20MW, the investigation delves into the temperature characteristics of smoke within the tunnel and its effect on vertical shaft smoke extraction. Findings reveal consistent longitudinal temperature profiles of smoke along the tunnel ceiling across varying conditions, with relatively higher ceiling temperatures in low-pressure environments. The ceiling's peak temperature in the fire source area varies with the power of the heat source, demonstrating a decrease in the highest longitudinal temperature as ambient pressure diminishes. Smoke temperature profiles at different tunnel locations remain fundamentally consistent, showing increased temperatures in low-pressure settings, with fire source sections exhibiting higher temperatures than non-source sections. At lower heat source powers, substantial temperatures persist at the 2m height level within the fire source area. The maximum smoke temperature differences upstream and downstream of the vertical shaft approximate 100℃, with shaft temperatures also escalating as pressure decreases. In low-pressure environments, the shaft's extraction capacity weakens, enhancing smoke evacuation efficiency. The results from studying tunnel fires in low-pressure environments provide valuable insights for practical tunnel design, evacuation strategies, and firefighting rescue operations.

1. INTRODUCTION

Since the implementation of the Western Development policy, rapid progress has been observed in China's western regions, particularly in the construction of highways and railways infrastructure, which has been increasing annually [1, 2]. The prevalence of mountains and the rising altitude in these western areas pose significant challenges to tunnel construction. An increase in altitude results in variations in atmospheric pressure and air density. The relationship between ambient pressure and altitude is described by Eq. (1), where p_h represents the atmospheric pressure at an altitude of h meters, measured in Pascals (Pa) [3]:

$$p_h = 101325 \times \left(1 - \frac{h}{44329}\right)^{5.255876} \quad (1)$$

Calculated using this formula, the relationship between atmospheric pressure and altitude is illustrated in Figure 1. This relationship is nonlinear, with ambient pressure decreasing as altitude increases. Taking China's topography as an example, the average altitude of the Northeast Plain, North China Plain, and the middle and lower reaches of the Yangtze River is below 500 meters, where the ambient pressure is around 100 kPa. In regions like the Loess Plateau, Yunnan-Guizhou Plateau, and the Inner Mongolia Plateau, with average altitudes ranging from 1000 to 2000 meters, the ambient pressure lies between 80 and 90 kPa. In the Tibetan region of the Qinghai-Tibet Plateau, with an average altitude exceeding 4000 meters, the ambient pressure falls below 60 kPa.
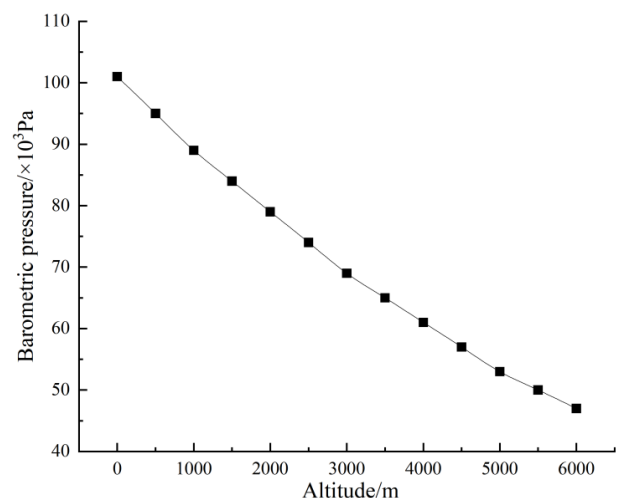

Figure 1. Atmospheric pressure at different altitudes

Eq. (2) presents the expression for environmental air density in relation to pressure (P) and temperature (T), as referenced in literature [4]. Both the external temperature and ambient pressure decrease with increasing altitude. Moreover, the rate of change in temperature is less pronounced than that of pressure. Consequently, the environmental air density diminishes alongside the reduction in ambient pressure. Therefore, as altitude increases and pressure decreases, air density lowers, leading to thinner air, which can result in an increased likelihood of hypoxia for individuals.

$$\rho = 3.48 \times 10^3 \frac{P}{T} \qquad (2)$$

The low atmospheric pressure, reduced oxygen content, and thin air in high-altitude regions not only present challenges to construction personnel but also make smoke dispersion and temperature field changes in tunnel fires a focal point of research both domestically and internationally in recent years. In high-altitude areas, tunnel fires tend to spread more rapidly than in plain areas due to lower pressure and less air resistance. Additionally, the semi-enclosed structure of tunnels, combined with the hypoxic state in high-altitude regions, significantly complicates evacuation efforts during tunnel fires. Therefore, conducting research on tunnel fires in high-altitude areas is crucial for tunnel ventilation design and smoke control to ensure the safety of lives and property.

Scholars both domestically and internationally have conducted extensive research on the characteristics of smoke from tunnel fires in high-altitude areas. Tang et al. [5] utilized the FDS software to compare smoke temperature and CO concentration in tunnel fires near sea level (1atm) and in high-altitude areas (0.64atm). They discovered that the longitudinal attenuation curve of CO concentration in smoke is independent of ambient pressure, whereas temperature attenuation occurs more rapidly under low pressure conditions. Ji et al. [6, 7] conducted a series of simulations in full-scale highway tunnels to explore the impact of ambient pressure on smoke movement and temperature distribution in tunnel fires. Their results indicated that with decreasing ambient pressure, the smoke spread distance from the fire source increases, and the longitudinal temperature curve rises due to reduced air density and entrainment strength, leading to a decrease in smoke mass flow rate with reduced ambient pressure. Yan et al. [8] conducted six large-scale fire experiments in a tunnel at an altitude of 4100 meters, finding that the smoke temperature distribution curve along the tunnel ceiling in high-altitude fires is consistent with that at lower altitudes. The longitudinal temperature attenuation rate near the fire source on the tunnel ceiling was significantly faster than at more distant points on either side of the source. Yan et al. [9-11] conducted a series of numerical simulations in highway tunnels under varying heat release rates and ambient pressures, demonstrating that in low-pressure environments, the vertical temperature rate of smoke is higher and the longitudinal distribution of smoke temperature in the tunnel increases as ambient pressure decreases. The counter flow distance of smoke is higher in low-pressure environments, and the counter flow length remains unchanged when the heat release rate is large. Additionally, studies on the movement pattern of shaft smoke in high-altitude environments revealed that reduced ambient pressure, leading to increased smoke temperature and velocity, results in a lower critical Richardson number (Ri) [12]. Liu et al. [13, 14] used FDS to simulate tunnel fires at different heat release rates and altitudes, finding that smoke movement speed increases with altitude, and smoke in high-altitude areas exhibits faster longitudinal temperature attenuation. The higher the altitude, the lower the flame temperature rise, while the opposite is true for plume temperature rise. Wang et al. [15] conducted a series of tunnel fire simulations by varying ambient pressure, fire heat release rate, and longitudinal wind speed, finding that reduced ambient pressure enhances the longitudinal distribution differences in CO concentration and smoke temperature, and smoke extraction efficiency of shafts increases slowly with decreasing ambient pressure. Yao et al. [16] conducted numerical studies on the impact of ambient pressure on tunnel fire smoke movement, finding that ambient pressure affects the buoyancy of the smoke plume at the front of the smoke backlayer, with critical wind speed negatively correlated with ambient pressure. Wang et al. [17] conducted small-scale fire experiments in high-altitude areas, revealing that the maximum ceiling smoke temperature in tunnels decreases with increasing altitude, and high-altitude diesel pool fires produce higher CO concentrations.

As discussed above, ambient pressure significantly influences the temperature distribution and movement characteristics of smoke in tunnel fires. However, most studies focus on single fire source scenarios, with limited research on dual or multiple fire sources. In real-life situations, fires in high-altitude areas are likely to involve multiple vehicle fires due to factors like rapid smoke spread and high tunnel radiant temperatures, leading to multi-source fire incidents. The impact of multi-source fires on smoke dispersion and thermal radiation in tunnels differs considerably from single-source fires. Therefore, this study employs FDS software for numerical simulation research, adjusting the combustion release rate and ambient pressure of dual fire sources to investigate fire scenarios in naturally ventilated tunnels at high altitudes. The study analyzes the differences in smoke dispersion, temperature distribution, and the efficiency of vertical shaft smoke extraction in dual-source fires at different altitudes, providing insights for fire prevention and control in high-altitude highway tunnels.

2. MODEL AND METHODS

2.1 FDS

The FDS, developed by the National Institute of Standards and Technology (NIST) in the United States, is a Computational Fluid Dynamics (CFD) model [18]. It employs turbulence models based on Large Eddy Simulation (LES) and Direct Numerical Simulation (DNS) to simulate energy-driven fluid flow in fires. FDS is commonly used for smoke control studies, sprinkler system research, and fire simulation experiments in civilian buildings and underground spaces. The software's experimental simulation results have been validated and accepted by many scholars, confirming its accuracy in predicting fire smoke dispersion [19, 20].

2.2 Model establishment

A vertical shaft tunnel model was established in FDS, as shown in Figure 2. The design of the highway tunnel is 120m×10m×5m (length x width x height). The vertical shaft is located 50m from the right opening of the tunnel and has a

height of 5m, with a shaft opening cross-sectional area of 2m×2m. The lining of the shaft and tunnel is made of concrete. The sides of the tunnel and the top of the shaft are open to the external environment. Fire Source A is positioned 47m from the left opening of the tunnel, and Fire Source B is located 20m to the left of the shaft, with a 3m distance between the two sources and aligned on the central line of the tunnel floor. The fire sources are modeled as n-heptane, and the fire model is a t² non-steady-state ultra-fast fire.
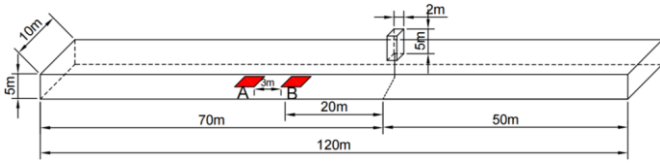

Figure 2. Geometric model of the tunnel

Thermocouples are installed 10 centimeters below the ceiling at 1-meter intervals for measuring the temperature of the smoke at the tunnel ceiling. Inside the shaft, between the two fire sources, and 10 meters to either side of the shaft, thermocouples are vertically arranged at 20-centimeter intervals. These are used for measuring the vertical temperature of smoke in both the fire source and non-fire source sections. At the shaft opening, measurement points for CO volume fraction and a mass flow measurement plane are set up to assess the effectiveness of smoke extraction through the shaft.

3. PARAMETER SETTINGS

3.1 Case setup

Table 1. Oxygen content at different pressures

Ambient Pressure (kPa)	Oxygen Mass Fraction (kg/kg)
60	0.160
70	0.180
80	0.199
90	0.216
101	0.232

Table 2. Case settings

Case	Power of Fire Source A (MW)	Power of Fire Source B (MW)	Ambient Pressure (kPa)
1-5	5	5	
6-10	5	10	60/70/80/90/101
11-15	5	20	
15-20	10	5	

Referring to the heat release rates for different types of vehicle fires given by the National Fire Protection Association (NFPA) 502, and considering the common types of vehicles in highway tunnels, this experiment selects three different fire source powers: 5MW, 10MW, and 20MW, representing the combustion power of cars, trucks, and buses, respectively. Based on the terrain distribution characteristics of China discussed earlier, five altitudes ranging from 0 to 4000 meters

are chosen, with corresponding simulated ambient pressures of 60, 70, 80, 90, and 101 kPa. Table 1 lists the oxygen content corresponding to different ambient pressures, with an ambient temperature set at 20℃ (although in actual areas, the temperature decreases with increasing altitude). Table 2 details the 20 scenarios set up for the numerical simulation, to study the characteristics of smoke temperature distribution in naturally ventilated tunnel fires under different dual fire source heat release rates and ambient pressures, as well as their impact on smoke extraction through vertical shafts.

3.2 Grid setting

In FDS experiments, the size of the grid set determines the accuracy of the simulation results. Smaller grid sizes result in less fluctuation in the calculated results, smoother simulation curves, and higher precision. However, this demands more from computer hardware and lengthens the simulation time. Conversely, overly large grid sizes, while saving time, lead to greater fluctuations in results, affecting the experiment's accuracy and scientific reliability.

Referring to the independent grid size tests by McGrattan et al. [21], the fire characteristic diameter D^* is a key parameter in evaluating grid size. A ratio of D^* to tunnel grid size δ_x generally falling between 4 and 16 ensures accurate computation of fluid viscous stress. The expression for D^* is as follows:

$$D^* = \left(\frac{Q}{\rho_0 c_p T_0 g^{1/2}} \right)^{2/5} \tag{3}$$

where, Q is the heat release rate of the fire source, measured in kW; ρ_0 is the environmental air density, in kg/m³; c_p is the specific heat capacity of air, in kJ/(kg·K); T_0 is the environmental temperature, in K; and g is the gravitational acceleration, in m/s².
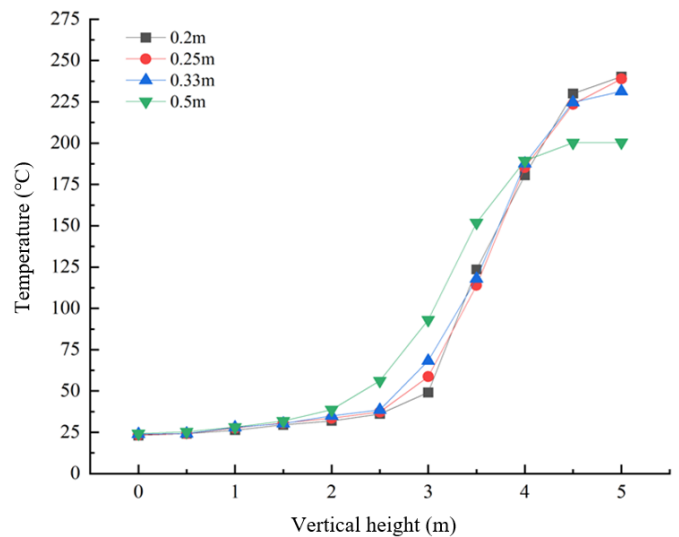
3.3 Grid sensitivity analysis

Figure 3. Vertical temperature distribution at 10m from the fire source

Prior to the simulation experiments, a grid independence analysis is conducted to verify the independence of the grid. For this study, a case with dual fire source power of 5MW each,

and an ambient pressure of 60kPa, was chosen. According to Eq. (3), the corresponding grid size range is calculated to be between 0.1 and 0.5 meters. Four different grid sizes were selected for simulation: 0.2m, 0.25m, 0.33m, and 0.5m. The temperature changes in the vertical direction within the tunnel under these different grid sizes were observed. As shown in Figure 3, when the grid size is less than 0.33 meters, the temperature differences are not significant. Considering the computer performance and time required for the experiment, the final grid size was set at 0.33 meters, with the total number of grids in the overall tunnel model being approximately 160,000.

4. SIMULATION RESULTS ANALYSIS

4.1 Smoke dispersion

In the initial stages of a tunnel fire, the smoke near the fire source undergoes three-dimensional diffusion and flow. The smoke plume formed by the fire source primarily spreads towards the tunnel ceiling, then disperses horizontally along the ceiling in a one-dimensional motion, eventually leading to the smoke sinking in areas farther from the fire source over time. To analyze the influence of different altitudes and ambient pressures on the dispersion pattern of smoke from dual fire sources in tunnels, cases 6-10 from this study are taken as examples. In these cases, the upstream fire source A is 5MW, and the downstream fire source B is 10MW, simulated under five different ambient pressures, as shown in Figure 4. In the absence of longitudinal wind, the lower the pressure, the closer the smoke spreads to the tunnel exit, and the relatively faster the spreading speed.
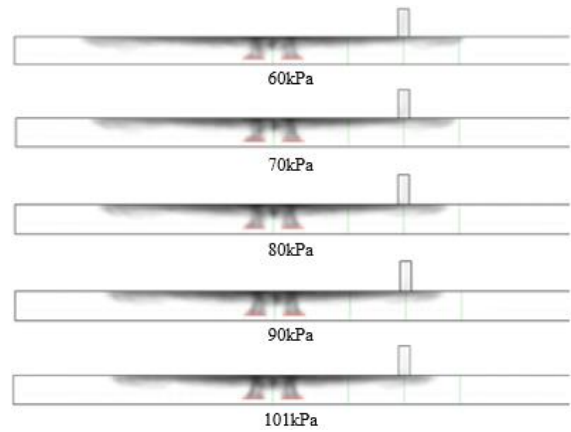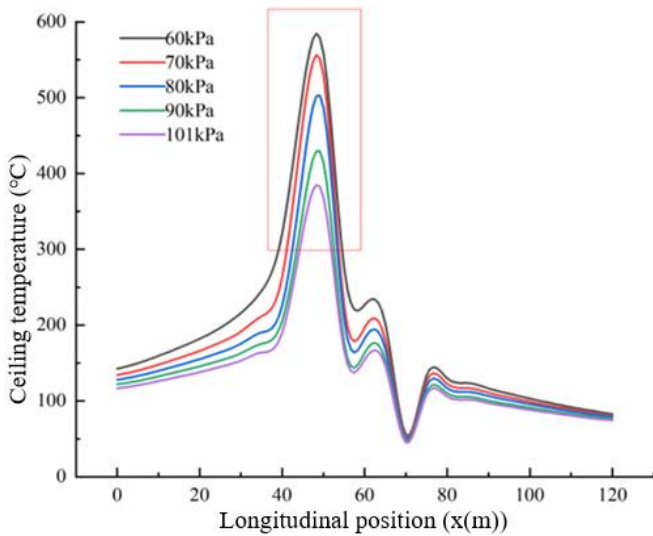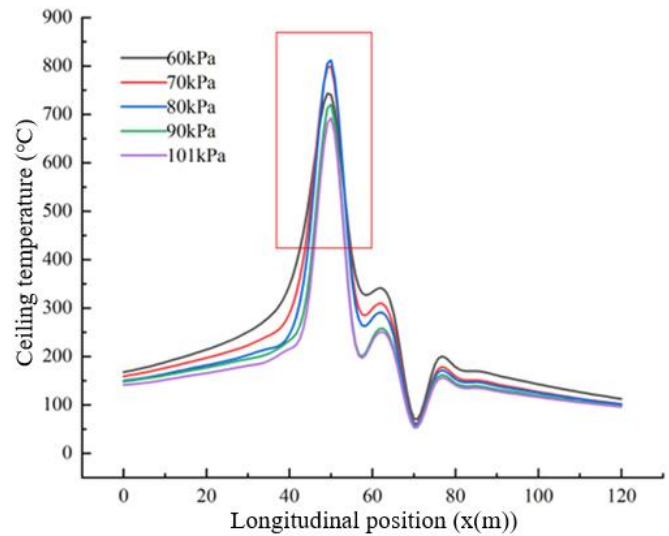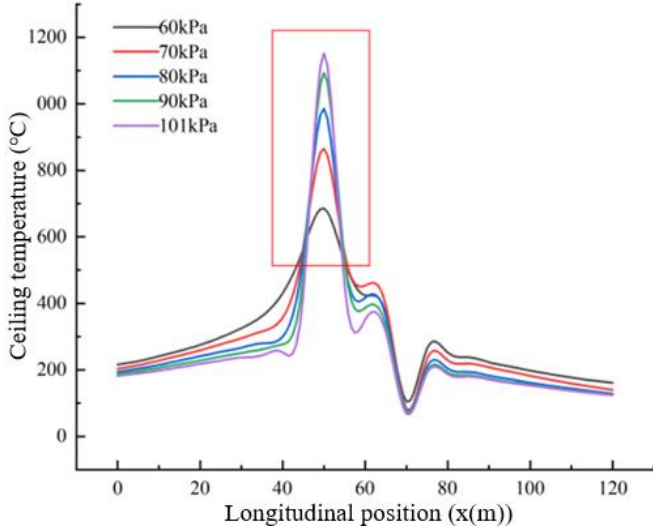

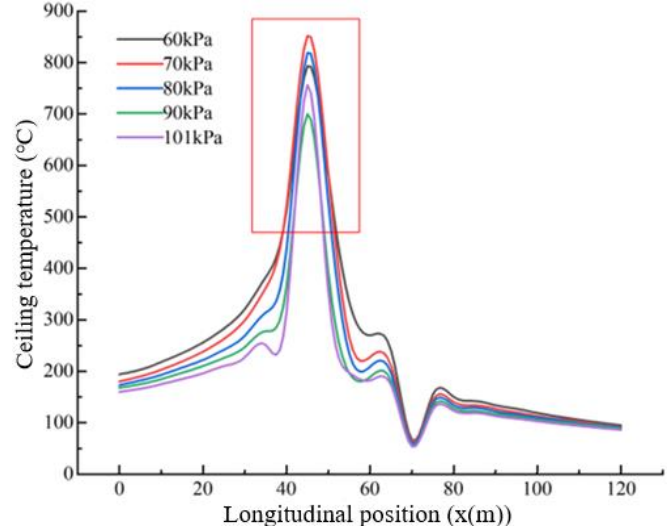**Figure 4.** Smoke spread in the tunnel

(a) Fire source power 5MW, 5MW

(b) Fire source power 5MW, 10MW

(c) Fire source power 5MW, 20MW

(d) Fire source power 10MW, 5MW

Figure 5. Tunnel ceiling temperature under different ambient pressures and fire source heat release rates

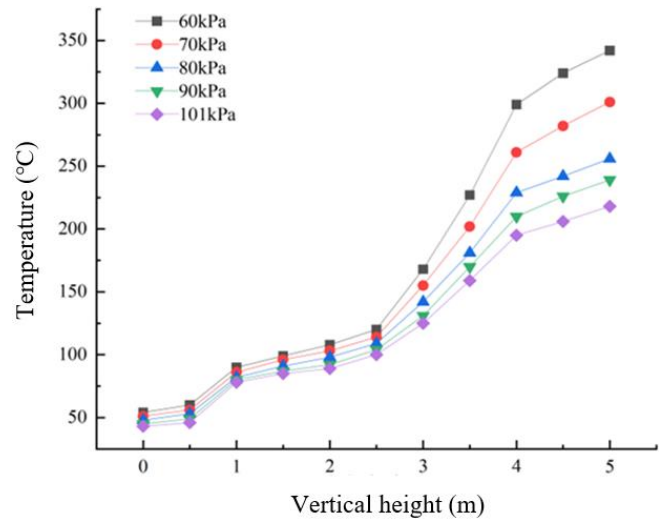## 4.2 Longitudinal temperature distribution of smoke

The longitudinal temperature distribution along the tunnel ceiling and the highest temperatures near and above the fire sources, which could lead to the spalling of lining concrete and potentially result in tunnel abandonment, are issues of interest to many scholars [22-24]. Figure 5 shows the longitudinal temperature distribution along the tunnel ceiling under different fire source powers and ambient pressures. As non-steady-state fire sources are used, the temperature data in the figure represent average values after the heat release rate of the fire source stabilizes. It is evident from the figure that the temperature distribution curves simulated under different fire source powers and ambient pressures are essentially the same. The closer to the fire source, the higher the temperature, and the further from the fire source, the lower the temperature. The longitudinal temperature distribution curve of the tunnel ceiling initially increases, then decreases, and finally reaches a relatively stable stage. The rate of temperature rise near the fire source is much greater than that upstream of the fire source, and the longitudinal temperature attenuation speed near the fire source is significantly faster than downstream, a conclusion consistent with Yan's fire experiment results [8]. The lowest temperature occurs at the shaft opening (70m), indicating that the chimney effect of the shaft helps to expel fire smoke from the tunnel, thus having a cooling effect. Besides the changes in ceiling temperature near the fire source area, the longitudinal temperature change along the tunnel ceiling increases as ambient pressure decreases.
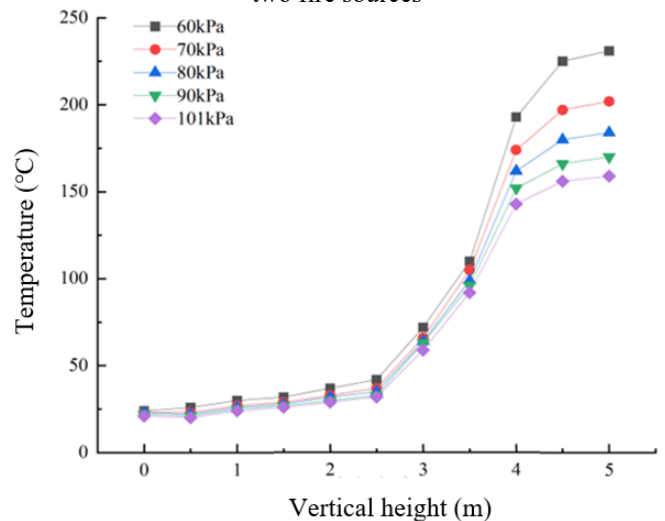
4.3 Vertical temperature distribution of smoke

The vertical temperature in the tunnel is used to calculate the smoke layer thickness and is a crucial factor in smoke stratification [25]. To explore the vertical temperature distribution at different positions in the tunnel under various ambient pressures, data was processed for a case with both fire sources at 5MW, as shown in Figure 6. Overall, the vertical temperature change curves at different positions in the tunnel are similar, with temperatures increasing with vertical height. Lower ambient pressure environments exhibit higher temperatures. This is because a decrease in ambient pressure leads to reduced air density and entrainment, resulting in lesser heat loss from the smoke and a slower rate of temperature attenuation compared to normal atmospheric pressure. The chimney effect of the shaft expels part of the smoke, significantly lowering temperatures downstream. Additionally, the remaining smoke spreads outward after passing the shaft opening, exchanging some heat with the cooler air and tunnel walls inside the tunnel, leading to lower temperatures in the downstream area of the shaft compared to the fire source section.

In the fire source area, the highest ceiling temperature under a 60kPa ambient pressure reaches nearly 350°C due to the combined effect of both fire sources, which is about 120°C higher than at the same height under normal atmospheric pressure. The temperature rises slowly from 0m to 2.5m in vertical height, and rapidly increases above 2.5m, indicating this height reaches the smoke layer. According to relevant sources, the safe evacuation condition for people in fire areas is that the environmental temperature at the human characteristic height of 2m should be less than 60°C [26]. The temperature at 2m vertical height between the two fire sources is close to 100°C, which is relatively high. At other positions,
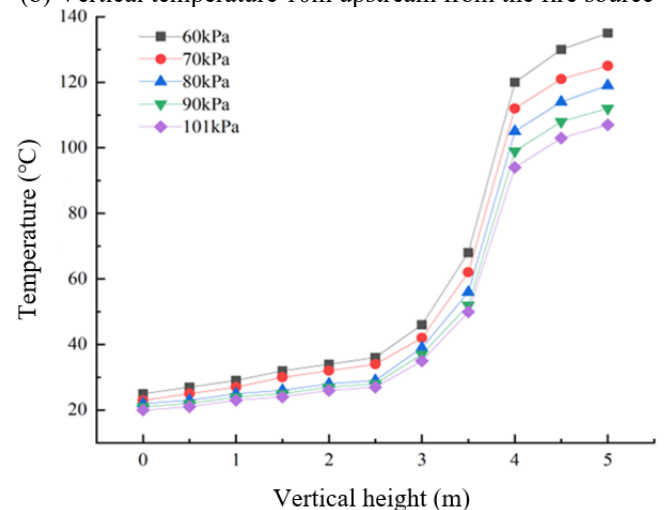
the temperature at 2m vertical height is below 60°C, with even lower temperatures in the downstream area of the shaft. In the event of a fire, people should evacuate as quickly as possible away from the fire source and, if feasible, move towards the downstream direction of the shaft.

(a) Vertical temperature at the central position between the two fire sources

(b) Vertical temperature 10m upstream from the fire source

(c) Vertical temperature 10m to the right of the shaft

Figure 6. Vertical temperature variations at different positions within the tunnel
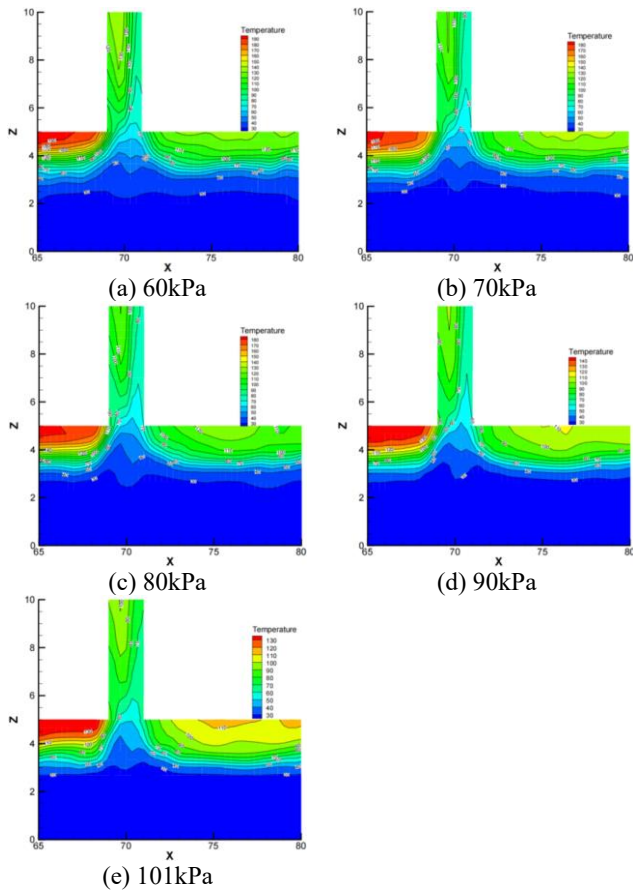
Figure 7. Temperature field in the tunnel and shaft with fire source powers of 5MW and 5MW
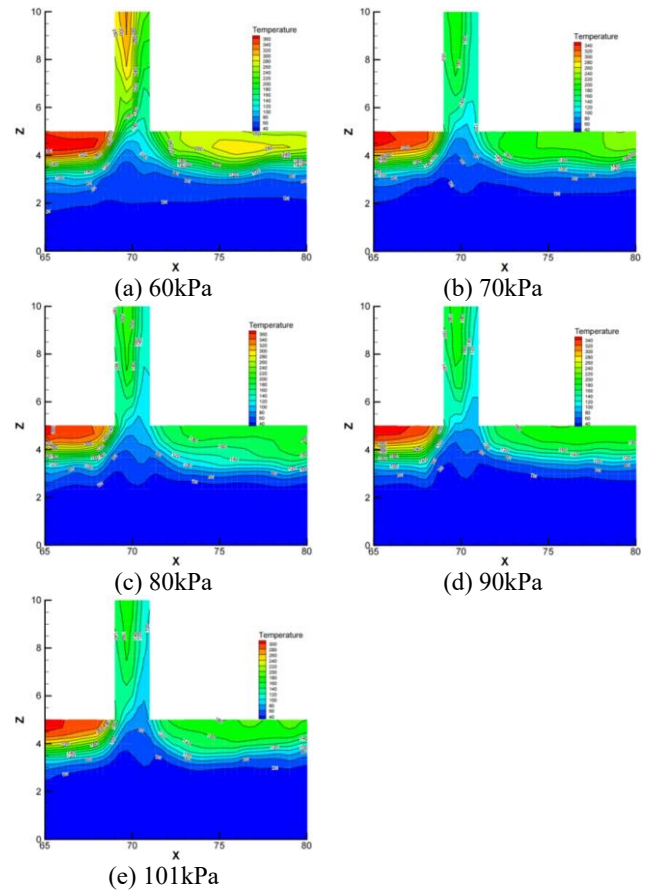

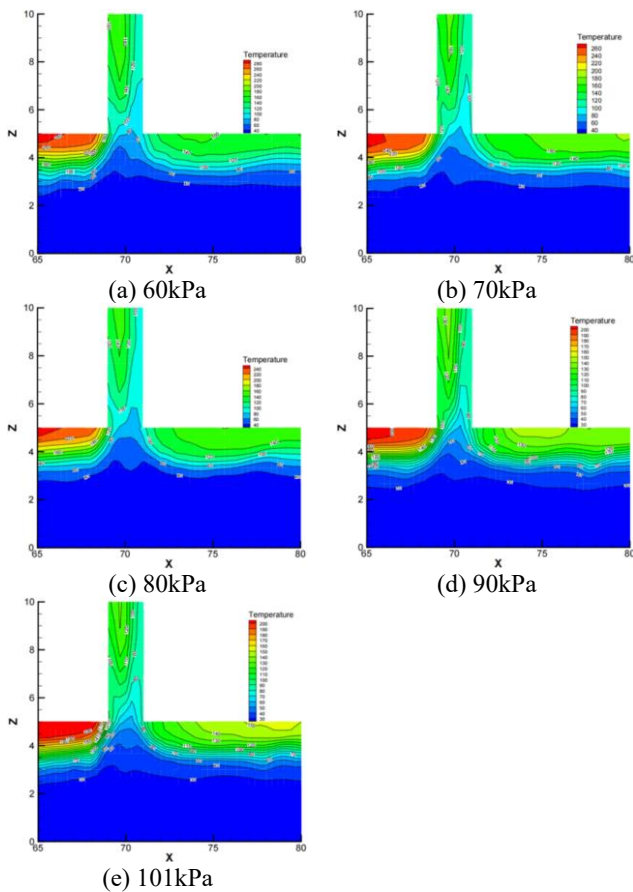**Figure 8.** Temperature field in the tunnel and shaft with fire source powers of 5MW and 10MW

Figure 9. Temperature field in the tunnel and shaft with fire source powers of 5MW and 20MW

4.4 Temperature field distribution in the shaft

The establishment of a shaft in a tunnel creates a pressure difference between the inside and outside of the tunnel, leading to a chimney effect. Part of the smoke produced by the fire is expelled through the shaft. The Figures 7-9 shows the temperature distribution within the shaft and its nearby area, examined by varying the heat release rate of the downstream fire source B and under different ambient pressure conditions. It is observed that under the same fire source power condition, the temperature in and around the shaft increases as the ambient pressure decreases. At the same ambient pressure, a higher fire source power results in higher smoke temperatures, consistent with the previous discussion on longitudinal smoke temperature distribution. Due to the chimney effect of the shaft, there is a significant temperature difference between the upstream and downstream temperatures of the shaft. For example, with a fire source B power of 20MW, regardless of standard or low-pressure environments, the smoke temperature difference between the upstream and downstream of the shaft is about 100°C, demonstrating the significant effect of the shaft smoke exhaust system in controlling smoke from tunnel fires.

The temperature cloud map of the shaft reveals a "dipping" of cooler air into the shaft at the shaft opening, caused by the chimney effect of the shaft, where the vertical buoyancy of the smoke is greater than the horizontal inertial force, resulting in a cold air entrainment phenomenon. Yan's study on the motion pattern of shaft smoke in high-altitude, low-pressure environments found that under standard atmospheric pressure, the entrainment effect in the shaft occurs when the Ri number is greater than 1.4 [11]. As the ambient pressure decreases, the

critical Ri number also decreases. The Ri number is used to determine the smoke movement pattern in the shaft, which is influenced by the ratio of vertical buoyancy to horizontal inertial force. The expression for Ri is as follows:

$$Ri = \frac{\Delta \rho g h A}{\rho_s v^2 dw} \qquad (4)$$

where, $\Delta \rho$ represents the density difference between the smoke and air in the shaft, in kg/m³; g is the gravitational acceleration, in m/s²; h is the height of the shaft, d is the thickness of the smoke under the shaft, w is the width of the shaft, in meters; A is the area of the shaft, in m^2; ρ_s is the density of the smoke under the shaft, in kg/m³; and v is the velocity of the smoke under the shaft, in m/s.

5. DISCUSSION

5.1 Smoke velocity

Table 3 presents the time taken for fire smoke from upstream fire source 5MW and downstream fire source 10MW to spread to both ends of the tunnel under different ambient pressures in cases 6-10. The table indicates the counter flow distance of the smoke, measured as the distance the smoke spreads along the ceiling from upstream fire source A to the left side of the tunnel after 60 seconds of the fire incident. It is evident from Table 3 that the time taken for smoke to reach the right end of the tunnel is significantly longer than that to the left end. This is firstly due to the fire sources not being positioned in the center of the tunnel but skewed towards the left, and secondly, due to the ventilation shaft on the right side of the tunnel which creates a chimney effect, causing part of the smoke to be expelled and slowing down the smoke spread. Regardless of whether the smoke spreads to the left end or towards the right end with the shaft, the time to reach the end decreases with decreasing ambient pressure, and the counter flow distance increases as the pressure decreases.

The smoke spread velocity increases with increasing altitude, a trend consistent with the findings of literatures [13, 14]. As derived from Eq. (5) for pressure, it can be concluded that under a constant contact area S, a decrease in atmospheric pressure P means a reduction in the air pressure force F on the smoke. If the smoke encounters less air resistance during its spread, its velocity increases. Therefore, smoke generated by fires in tunnels at higher altitudes spreads faster than in plains areas. This underscores the need for enhanced early smoke detection sensitivity and improved evacuation capabilities in tunnel designs in high-altitude areas.

$$P = \frac{F}{S} \qquad (5)$$

Table 3. Smoke spread under different ambient pressures

Ambient Pressure (kPa)	Time for Smoke to Spread to Left End (s)	Time for Smoke to Spread to Right End (s)	Counter flow Distance (m)
60	76.3	113.2	27
70	78.8	116.6	25
80	81.2	118.9	23
90	83.8	123.1	22
101	85.8	125.9	21

5.2 Ceiling temperature in the fire source area

To more clearly study the longitudinal ceiling temperature and the highest temperature pattern in the tunnel fire source area, Figure 10 shows the temperature changes within the fire source area under different fire source powers. From Figure 10, it is evident that the higher smoke temperatures near the ceiling above the fire source and in the nearby area are closely related to fire behavior under different atmospheric pressure conditions. In lower ambient pressure, the combined effects of increased flame volume and reduced smoke production lead to reduced radiant heat loss during combustion, thus increasing the flame temperature and consequently the smoke temperature at the tunnel ceiling. For different fire source powers burning under the same pressure, if the power of fire source A remains constant while that of fire source B increases, the heat radiated from the thermal release will be greater, resulting in higher smoke temperatures, and the highest ceiling temperature in the fire source area will increase.

Due to air entrainment between the dual fire sources, causing slight flame deviation, the highest ceiling temperature point is not located at the center of the fire source. A comparison of Figure 10(b) and Figure 10(d) shows that switching the powers of the dual fire sources has little impact on the ceiling temperature of the tunnel, only changing the position of the highest temperature point. A comparison of Figure 10(a) and Figure 10(c) reveals that the pattern of the highest longitudinal temperature of the ceiling changes under different atmospheric pressures with the variation in fire source power. A larger fire source power results in a decrease in the highest longitudinal ceiling temperature as ambient pressure decreases. This may be due to a significant increase in flame height with larger fire source powers (the flame height of a larger heat release rate fire source is higher than the flame expansion height under low pressure), bringing it closer to the tunnel ceiling. Additionally, combustion requires more oxygen, and the oxygen content increases at relatively higher pressures, resulting in higher temperatures in the fire source area under higher pressures. The impact of ambient pressure and fire source power on flame height will be further studied in subsequent experiments.

5.3 Efficiency of shaft smoke exhaust

To investigate the efficiency of smoke exhaust through the shaft under different ambient pressures, numerical simulations were conducted to study the variations in gas mass flow and CO concentration expelled by the shaft at different pressures. Figures 11 and 12 present the line charts showing changes in the mass flow of gases and CO concentration in the shaft under varying ambient pressures. From Figure 11, it is evident that the trend of the mass flow of gases expelled by the shaft under

different fire source powers is similar, increasing with higher ambient pressures. The mass of gases expelled by the shaft also increases with the increase in fire source power, and a larger fire source power causes a greater curvature in the shaft mass flow curve, indicating enhanced exhaust capability. For dual fire sources at 5MW and 10MW, the gas mass flow in the shaft at 60kPa is 13.3 kg/s, compared to 20.5 kg/s under normal pressure, an increase of about 35% in a low-pressure environment.
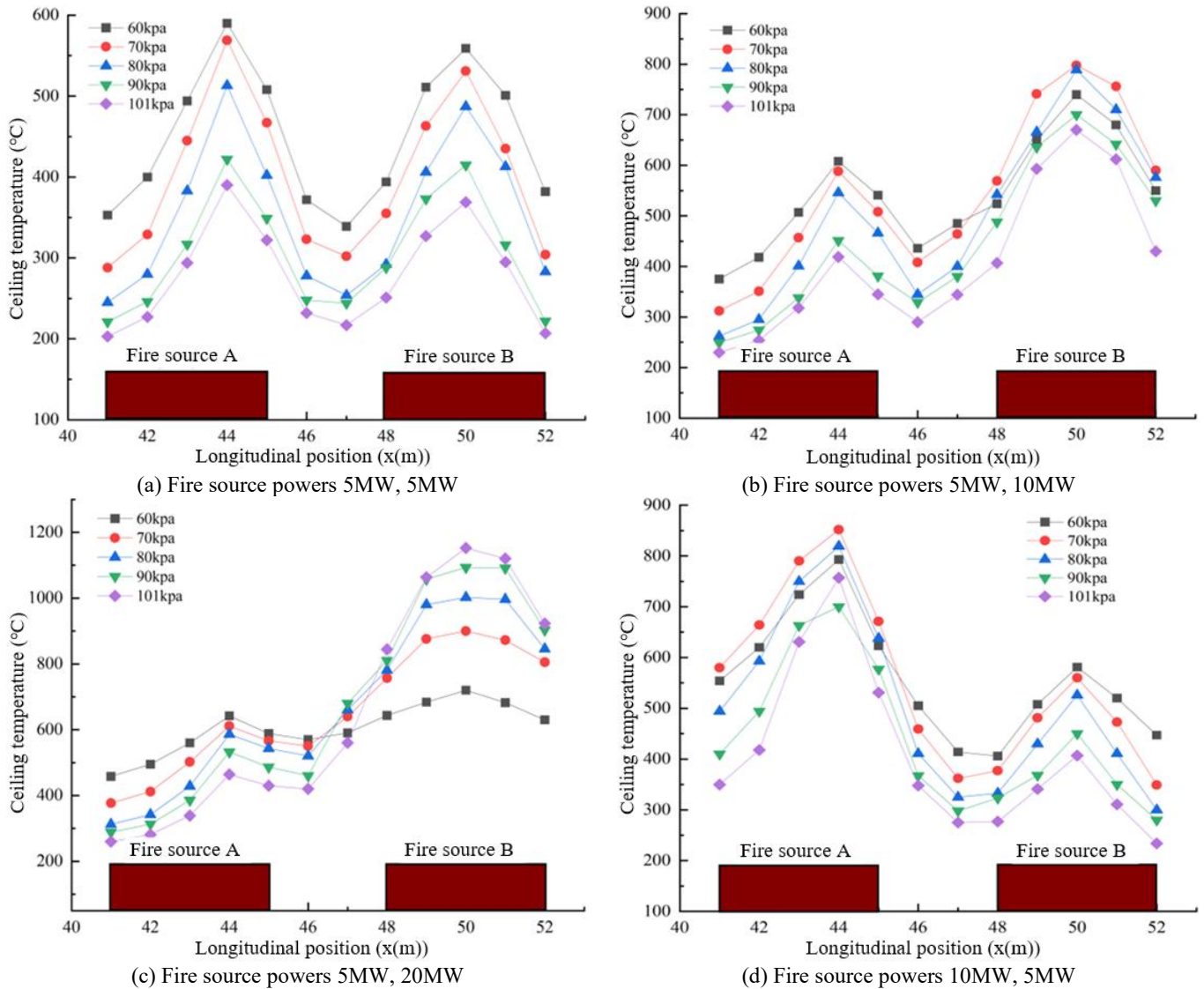

(a) Fire source powers 5MW, 5MW

(b) Fire source powers 5MW, 10MW

(c) Fire source powers 5MW, 20MW

(d) Fire source powers 10MW, 5MW

Figure 10. Temperature changes at the tunnel ceiling in the fire source area
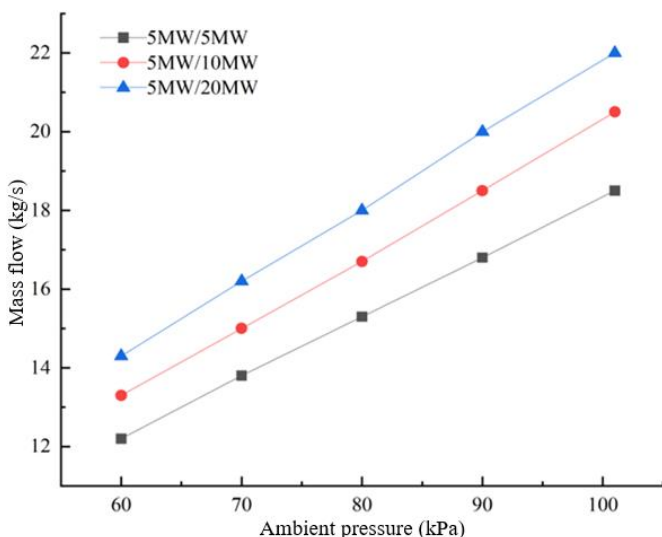

Figure 11. Gas mass flow under different ambient pressures

The entrainment effect at the shaft exhaust can expel some fresh air, reducing the efficiency of smoke exhaust. Since the amount of CO in normal air is negligible, studying the amount of CO expelled by the shaft provides a more accurate reflection of exhaust efficiency. With changes in ambient pressure, the CO concentration in the shaft also shows a certain pattern. As shown in Figure 12, the CO concentration expelled by the shaft increases as ambient pressure decreases, with larger fire source powers causing a greater curvature in the expelled CO concentration. With a constant fire source power, taking dual fire sources at 5MW and 10MW as an example, the CO concentration expelled by the shaft at 60kPa is about 26% higher than under normal pressure.

As atmospheric pressure increases, air density increases, leading to a higher mass of cold air at the bottom of the tunnel. This results in greater heat and mass exchange between the upper smoke and the lower fresh air, enhancing the chimney effect of the shaft and expelling more fresh air. Analyzing solely based on CO concentration changes, the efficiency of

smoke exhaust through the shaft increases with decreasing ambient pressure, consistent with the findings of literature [15]. Changes in ambient pressure can impact the critical height required for complete smoke exhaust through the shaft. Researcher Zhao [27] found through simulation studies that ambient pressure has a dual effect on the chimney effect of the shaft, with the chimney effect weakening under low pressure, leading to an increase in the critical height of the shaft.
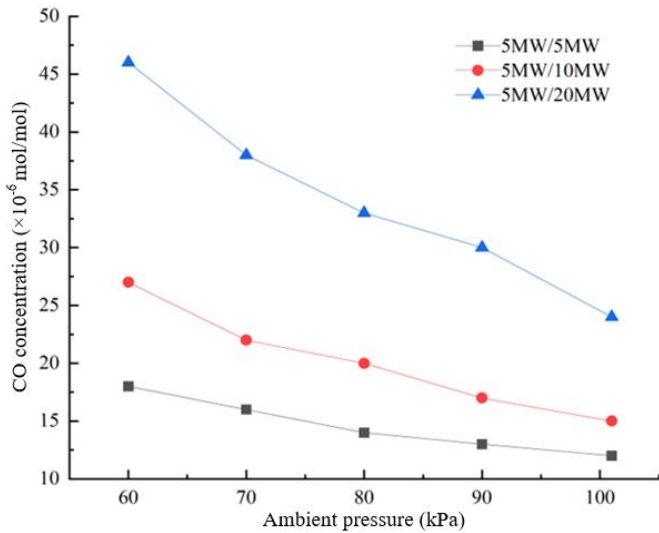

Figure 12. CO concentration under different ambient pressures

6. CONCLUSION

To study the development characteristics of smoke from dual fire source fires in tunnels at different altitudes, this study used the FDS software to simulate the temperature distribution of smoke in naturally ventilated shaft tunnels and its impact on shaft smoke exhaust under various dual fire source powers and ambient pressures. The main conclusions are as follows:

(1) The speed of smoke spread in tunnels increases with decreasing ambient pressure, posing a greater threat to personnel evacuation in dual fire source scenarios. Under different ambient pressures, the longitudinal smoke temperature characteristic curves in the tunnel are consistent, with ceiling smoke temperature increasing as atmospheric pressure decreases. Air entrainment between the dual fire sources causes flame temperature deviation. The ceiling temperature pattern in the fire source area changes with the fire source power under different atmospheric pressures, decreasing with increasing fire source power and decreasing ambient pressure.

(2) The vertical temperature distribution of smoke and the temperature within the shaft increase with decreasing ambient pressure. At a vertical height of 2.5m, the smoke temperature rises rapidly, suggesting that the smoke layer thickness is around 2.5m. The vertical temperature between the dual fire source areas is significantly higher than in other areas. The highest temperatures upstream and downstream of the shaft differ by about 100°C, indicating significant smoke exhaust effectiveness of the shaft.

(3) Under the same fire source scale, the mass flow in the shaft increases with increasing ambient pressure, while the CO concentration expelled by the shaft decreases. Increased ambient pressure enhances the chimney effect of the shaft,

expelling a larger amount of fresh air. At 60kPa, the CO concentration expelled by the shaft is about 26% higher than under normal pressure, indicating better smoke exhaust efficiency in a low-pressure environment. Changes in ambient pressure affect the critical height of the shaft, which will be a focus of our future research.

In summary, in high-altitude areas, tunnel fire smoke develops faster and reaches higher temperatures compared to plain areas, and dual fire source fires are more complex than single fire source fires. This simulation hopes to provide references for the study of dual fire source fires in high-altitude areas and for tunnel construction in such regions.

REFERENCES

[1] Wan, H., Jiang, Y., Jiang, J. (2023). A survey of fire accidents during the process of highway tunnel operation in China from 2010 to 2021: Characteristics and countermeasures. Tunnelling and Underground Space Technology, 139: 105237. https://doi.org/10.1016/j.tust.2023.105237

[2] Zhang, N., Tan, Z., Jin, M. (2015). Research on the technology of disaster prevention and rescue in high-altitude super-long railway tunnel. KSCE Journal of Civil Engineering, 19: 756-764. https://doi.org/10.1007/s12205-013-1248-2

[3] ASHRAE Research (2017). 2017 ASHRAE Handbook-Fundamentals. Atlanta, GA.

[4] Cao, Z., Liu, X., Niu, B. (2019). Migration characteristics of dust during construction stage in highway tunnels at high altitude areas. Chinese Journal of Underground Space and Engineering, 15(3), 927-935.

[5] Tang, F., Hu, L. H., Yang, L.Z., Qiu, Z.W., Zhang, X.C. (2014). Longitudinal distributions of CO concentration and temperature in buoyant tunnel fire smoke flow in a reduced pressure atmosphere with lower air entrainment at high altitude. International Journal of Heat and Mass Transfer, 75: 130-134. https://doi.org/10.1016/j.ijheatmasstransfer.2014.03.058

[6] Ji, J., Guo, F., Gao, Z., Zhu, J., Sun, J. (2017). Numerical investigation on the effect of ambient pressure on smoke movement and temperature distribution in tunnel fires. Applied Thermal Engineering, 118: 663-669. https://doi.org/10.1016/j.applthermaleng.2017.03.026

[7] Ji, J., Guo, F., Gao, Z., Zhu, J. (2018). Effects of ambient pressure on transport characteristics of thermal-driven smoke flow in a tunnel. International Journal of Thermal Sciences, 125: 210-217. https://doi.org/10.1016/j.ijthermalsci.2017.11.027

[8] Yan, Z.G., Guo, Q.H., Zhu, H.H. (2017). Full-scale experiments on fire characteristics of road tunnel at high altitude. Tunnelling and Underground Space Technology, 66: 134-146. https://doi.org/10.1016/j.tust.2017.04.007

[9] Yan, G., Wang, M., Yu, L., Tian, Y., Guo, X. (2020). Study of smoke movement characteristics in tunnel fires in high‐altitude areas. Fire and Materials, 44(1): 65-75. https://doi.org/10.1002/fam.2770

[10] Yan, G., Wang, M., Yu, L., Tian, Y. (2020). Effects of ambient pressure on the critical velocity and back-layering length in longitudinal ventilated tunnel fire. Indoor and Built Environment, 29(7): 1017-1027. https://doi.org/10.1177/1420326X19870313

[11] Yan, G., Wang, M., Yu, L., Duan, R., Xia, P. (2020).

Effects of ambient pressure on smoke movement patterns in vertical shafts in tunnel fires with natural ventilation systems. Building Simulation, 13: 931-941. https://doi.org/10.1007/s12273-020-0631-4

[12] Ji, J., Gao, Z.H., Fan, C.G., Zhong, W., Sun, J.H. (2012). A study of the effect of plug-holing and boundary layer separation on natural ventilation with vertical shaft in urban road tunnel fires. International Journal of Heat and Mass Transfer, 55(21-22): 6032-6041. https://doi.org/10.1016/j.ijheatmasstransfer.2012.06.014

[13] Liu, B., Mao, J., Xi, Y., Hu, J. (2021). Effects of altitude on smoke movement velocity and longitudinal temperature distribution in tunnel fires. Tunnelling and Underground Space Technology, 112: 103850. https://doi.org/10.1016/j.tust.2021.103850

[14] Bin, L., Jun, M., Yanhong, X., Jiawei, H. (2023). Effect of altitude on vertical temperature distribution and longitudinal smoke layer thickness in long tunnel fires. Fire and Materials, 47(1): 16-27. https://doi.org/10.1002/fam.3065

[15] Wang, J., Kong, X., Fan, Y., Jiang, X., Lu, K. (2022). Reduced pressure effects on smoke temperature, CO concentration and smoke extraction in tunnel fires with longitudinal ventilation and vertical shaft. Case Studies in Thermal Engineering, 37: 102311. https://doi.org/10.1016/j.csite.2022.102311

[16] Yao, Y., Zhang, Y., Zhu, H., Han, Z., Zhang, S., Zhang, X. (2023). Effects of ambient pressure on characteristics of smoke movement in tunnel fires. Tunnelling and Underground Space Technology, 134: 104981. https://doi.org/10.1016/j.tust.2023.104981

[17] Wang, F., Dai, K., Liang, S., Xiong, T., Wang, Y. (2023). Experimental field study on smoke characteristics and CO concentration of high-altitude tunnel fires induced using gasoline and diesel. International Journal of Thermal Sciences, 194: 108559. https://doi.org/10.1016/j.ijthermalsci.2023.108559

[18] Huang, Y., Li, Y., Dong, B., Li, J., Liang, Q. (2018). Numerical investigation on the maximum ceiling temperature and longitudinal decay in a sealing tunnel fire. Tunnelling and Underground Space Technology, 72: 120-130. https://doi.org/10.1016/j.tust.2017.11.021

[19] Hwang, C.C., Edwards, J.C. (2005). The critical ventilation velocity in tunnel fires - A computer simulation. Fire Safety Journal, 40(3): 213-244. https://doi.org/10.1016/j.firesaf.2004.11.001

[20] Khattri, S. K. (2017). From small-scale tunnel fire simulations to predicting fire dynamics in realistic tunnels. Tunnelling and Underground Space Technology, 61: 198-204. https://doi.org/10.1016/j.tust.2016.10.010

[21] McGrattan, K.B., Forney, G.P., Floyd, J., Hostikka, S., Prasad, K. (2005). Fire dynamics simulator (version 4)--user's guide. Gaithersburg, MD, USA: US Department of Commerce, Technology Administration, National Institute of Standards and Technology.

[22] Gong, L., Jiang, L., Li, S., Shen, N., Zhang, Y., Sun, J. (2016). Theoretical and experimental study on longitudinal smoke temperature distribution in tunnel fires. International Journal of Thermal Sciences, 102: 319-328. https://doi.org/10.1016/j.ijthermalsci.2015.12.006

[23] Kashef, A., Yuan, Z., Lei, B. (2013). Ceiling temperature distribution and smoke diffusion in tunnel fires with natural ventilation. Fire Safety Journal, 62: 249-255. https://doi.org/10.1016/j.firesaf.2013.09.019

[24] Jia, Y., Fan, X., Zhao, X., Deng, Y., Zhu, X., Zhao, W. (2022). Investigation of the maximum tunnel ceiling temperature caused by two fires. International Journal of Thermal Sciences, 178: 107596. https://doi.org/10.1016/j.ijthermalsci.2022.107596

[25] Tanno, A., Oka, H., Kamiya, K., Oka, Y. (2022). Determination of smoke layer thickness using vertical temperature distribution in tunnel fires under natural ventilation. Tunnelling and Underground Space Technology, 119: 104257. https://doi.org/10.1016/j.tust.2021.104257

[26] Zhong, M., Shi, C., Tu, X., Fu, T., He, L. (2008). Study of the human evacuation simulation of metro fire safety analysis in China. Journal of Loss Prevention in the Process Industries, 21(3): 287-298. https://doi.org/10.1016/j.jlp.2007.08.001

[27] Zhao, G. (2023). Study on the influence of environmental pressure on the characteristics of natural ventilation smoke in vertical tunnel fires ventilation. Refrigeration & Air Conditioning, 37(4): 535-538.